Synthesis and evaluation of ethyleneoxylated and allyloxylated chalcone derivatives for imaging of amyloid *β* plaques by SPECT

Takeshi Fuchigami[a*], Yuki Yamashita[a], Mamoru Haratake[a], Masahiro Ono[b], Sakura Yoshida[a], Morio Nakayama[a*]

[a] Department of Hygienic Chemistry, Graduate School of Biomedical Sciences, Nagasaki University, 1-14 Bunkyo-machi, Nagasaki 852-8521, Japan

[b] Graduate School of Pharmaceutical Sciences, Kyoto University, 46-29 Yoshida Shimoadachi-cho, Sakyo-ku, Kyoto 606-8501, Japan.

Abstract

We report radioiodinated chalcone derivatives as new SPECT imaging probes for amyloid *β* (A*β*) plaques. The monoethyleneoxy derivative **2** and allyloxy derivative **8** showed a high affinity for A*β*(1-42) aggregates with *K*i values of 24 and 4.5 nM, respectively. Fluorescent imaging demonstrated that **2** and **8** clearly stained thioflavin-S positive A*β* plaques in the brain sections of *Tg2576* transgenic mice. *In vitro* autoradiography revealed that [^{125}I]**2** displayed no clear accumulation toward A*β* plaques in the brain sections of *Tg2576* mice, whereas the accumulation pattern of [^{125}I]**8** matched with the presence of A*β* plaques both in

the brain sections of *Tg2576* mice and an AD patient. In biodistribution studies using normal mice, [^{125}I]**2** showed preferable *in vivo* pharmacokinetics (4.82%ID/g at 2 min and 0.45%ID/g at 60 min), while [^{125}I]**8** showed only a modest brain uptake (1.62%ID/g at 2 min) with slow clearance (0.56%ID/g at 60 min). [^{125}I]**8** showed prospective binding properties for Aβ plaques, although further structural modifications are needed to improve the blood brain barrier permeability and washout from brain.

Key words: Alzheimer's disease, amyloid β plaque, chalcone, single photon emission computed tomography (SPECT).

1. Introduction

Alzheimer's disease (AD) is the most common form of dementia in the elderly, characterized by memory loss and cognitive dysfunction. Amyloid β (Aβ) plaques and intracellular neurofibrillary tangles in the postmortem brain have been reported to be the key pathological hallmarks of AD[1,2]. According to the amyloid hypothesis, disruption of the balance between the production and clearance of Aβ leads to aggregation and accumulation of Aβ in the brain. This process may initiate various factors such as synaptic dysfunction for cognitive impairment in AD[3]. Non-invasive diagnostic methods, such as single photon emission computed tomography (SPECT) and positron emission tomography (PET), are

expected to be powerful tools for the detection of Aβ plaques in the early stage of AD and monitoring the efficacy of therapeutic treatments for AD patients. For these purposes, a number of Aβ plaques targeted *in vivo* imaging probes based on the dye staining for amyloid fibrils including thioflavin-T and Congo Red have been developed[4]. It has been demonstrated that several PET ligands could detect human brain Aβ plaques and distinguish AD patients from healthy subjects[5]. Recently, [^{18}F]florbetapir (Amyvid) and [^{18}F]flutemetamol (Vizamyl) were launched in the United States and/or Europe for the clinical evaluation of Aβ neuritic plaque density when evaluating patients with cognitive impairment[6,7]. SPECT imaging can provide a cost-effective and convenient approach for the visualization of Aβ plaques in the brain. Considerable effort has been devoted to the development of SPECT probes labeled with ^{99m}Tc or $^{123/125}$I for the Aβ plaques[8-13]. However, none of them have been approved by the Food and Drugs Administration (FDA) and/or the European Medicines Agency (EMA). [^{123}I]IMPY is the only SPECT imaging probe that has been used in clinical studies; however, the signal-to-noise ratio obtained for plaque labeling has been unsatisfactory[14]. Accordingly, there is real need for clinically useful SPECT probes for the detection of Aβ plaques.

We have previously reported Aβ imaging agents based on flavonoid derivatives, such as flavones[15,16], chalcones[17-20], aurones[21,22], and styrylchromones[23], for nuclear medicine imaging as shown in Fig. 1. Although several compounds have been demonstrated to be promising Aβ imaging probes, clinical studies of the compounds have not yet been conducted. Our previous

studies demonstrated that chalcone derivatives fluoro-pegylated at the *p*-position of the 1-phenyl ring showed a sufficient brain uptake with a good binding capacity to Aβ plaques[19]. In addition, radioiodinated flavonoids, such as flavone and aurone derivatives, with a methoxy or oligoethyleneoxy group at the *p*-position of the 3-phenyl ring have the properties of high brain uptake and rapid clearance from the brain without significant decrease in the binding affinity for Aβ[15,22]. On the basis of the results of these studies, we hypothesized that the introduction of ethyleneoxy groups at the *p*-position of the 3-phenyl ring or iodoallyloxy group at the *p*-position of the 1-phenyl ring in the chalcone derivatives could improve the binding affinity for the Aβ plaques and/or brain distribution pattern. In this paper, we report the additional structural modification of chalcone derivatives to discover useful imaging probes for Aβ plaques.

2. Results and discussion

2.1. Chemistry

The target chalcone derivatives were synthesized according to the procedure shown in Scheme 1. 4-Iodoacetophenone was reacted with 4-methoxybenzaldehyde in the presence of a basic catalyst (10% KOH) in ethanol at room temperature to form 4'-iodo-4-methoxy-chalcone **1** in quantitative yield. Direct alkylation of **1** with ethylene chlorohydrin, ethylene glycol mono-2-chloroethyl ether, or 2-[2-(2-chloroethoxy)ethoxy]ethanol with potassium

carbonate in DMF provided **2**, **3** and **4** for yields of 52, 49 and 17%, respectively. The tributyltin derivative **5** was prepared from the corresponding iodo derivative **4** using a iodo-to-tributyltin exchange reaction catalyzed by Pd(0) for a yield of 48%. The starting material **6** for the synthesis of the allyoxylated chalcone derivative **8** was prepared as previously reported[20]. The *p*-toluenesulfonate ester of (*E*)-3-(tri-*n*-butylstannyl)prop-2-enol[24] was coupled with the phenol **6** to produce the tributyltin derivative **7** in a yield of 45%. Compound **7** was reacted with iodine in $CHCl_3$ to form the target **8** (62% yield).

2.2. *In vitro* binding assays using A$\beta_{1–42}$ aggregates

In vitro binding experiments to evaluate the binding affinity of the chalcones for Aβ were performed in suspensions of Aβ (1-42) aggregates with [^{125}I]4-dimethylamino-4'-iodo-chalcone (DMIC) which is a high-affinity Aβ ligand with a chalcone backbone as described in our previous papers[17-20]. The inhibition constant (K_i) values of **2**-**4** indicated that the binding affinity of these compounds to Aβ aggregates was affected by the length of the ethyleneoxy group in the chalcone backbone. The rank order of their binding affinity for Aβ aggregates was as follows: monoethyleneoxylated derivative **2** (K_i= 24.0 nM) > triethyleneoxylated derivative **4** (K_i= 87.8 nM) > diethyleneoxylated derivative **3** (K_i = 127.1 nM). The *K*i value of **2** was significantly lower than those of **3** ($P < 0.001$; ANOVA, Bonferroni t test) and **4** ($P < 0.001$). The *K*i value of **4** was significantly lower than that of **3** ($P < 0.05$). The relationship

between the binding affinity and length of the oligoethyleneoxy group of the chalcones was similar to that of the aurone derivatives[22]. On the other hand, the allyloxy derivative **8** showed excellent binding affinity for Aβ (K_i= 4.5 nM), which is stronger than that of DMIC (K_i= 10.8 nM). Based on these *in vitro* results, we selected the monoethyleneoxy derivative **2** and allyloxy derivative **8** for further experiments.

2.3. Fluorescence staining on *Tg2576* mice brain sections

Fluorescence imaging experiments of the chalcones **2** and **8** were performed using brain slices from Aβ deposition model transgenic mice (*Tg2576* mice). A number of fluorescence spots of **2** and **8** were observed in the brain slices of the *Tg2576* mice (Figs. 2A and D). The labeling patterns of these compounds corresponded to the fluorescence signals obtained by thioflavin-S (Figs. 2B and E). In the wild-type mice brain, there was no significant fluorescence of **2** and **8** (Figs. 2C and F). The autofluorescence of the adjacent brain slices used in the assays was also examined. Significant fluorescence was not observed in any of the slices. These results indicated that **2** and **8** have specific binding potential to Aβ plaques in the mice brain.

2.4. *In vitro* autoradiography

The radioiodinated chalcones [^{125}I]**2** and [^{125}I]**8** were prepared by an iododestannylation

reaction using hydrogen peroxide as the oxidant (Scheme 2). [^{125}I]**2** and [^{125}I]**8** were obtained in radiochemical yields of 66−75% with radiochemical purities of > 95% after purification by HPLC. *In vitro* autoradiography of [^{125}I]**2** and [^{125}I]**8** was carried out using brain sections of the *Tg2576* mice. [^{125}I]**2** displayed no clear accumulation toward the Aβ plaques (Fig. 3A), while [^{125}I]**8** showed a distinctive plaque labeling with a low background (Fig. 3B). Labeled plaques by [^{125}I]**8** were matched with the thioflavin-S positive regions of the adjacent sections (Fig. 3C). It is possible that the differing concentration of **2** caused the discrepancy observed between the results of the fluorescence imaging and autoradiography studies: 100 μM of **2** was used for fluorescence staining, whereas only 0.3 nM of [^{125}I]**2** was used for autoradiography. On the other hand, this difference might be related to the binding affinity of the chalcone derivatives for the Aβ aggregates; **8** showed a 5.3-fold lower K_i value than **2** (Table 1). Indeed, it was reported that several Aβ probes with single-digit nanomolar K_i values for the Aβ aggregates successfully stained the Aβ plaques in brain sections of the *Tg2576* mice by *in vitro* autoradiography[25,26]. In addition, it has been shown that chalcone derivatives with a dimethylamino group at the third position can be used to visualize Aβ plaques by *in vitro* autoradiography[19,27]. Thus, chalcone derivatives with a dimethylamino group in the 3-phenyl ring may be more suitable than those with an alkoxy group with respect to binding of the Aβ plaques in the brain.

To further characterize the binding property of [^{125}I]**8** for the Aβ plaques, the *in vitro*

autoradiography of human AD brain sections was conducted. The autoradiogram of [^{125}I]**8** displayed a distinct accumulation of the radioactivity in the hippocampal section of the human brain (Fig. 4A), while no significant signals of [^{125}I]**8** were observed in the frontal lobe section of the brain (Fig. 4B). The labeled regions of [^{125}I]**8** corresponded to the immunohistochemical staining of Aβ in the hippocampal sections (Fig. 4C). Consistent with the autoradiographic image of [^{125}I]**8**, no Aβ plaques were detected in the frontal lobe section (Fig. 4D). These results strongly suggested that [^{125}I]**8** was bound to the Aβ plaques in the brain tissues.

2.5. *In vivo* biodistribution stuides

To develop prospective *in vivo* imaging probes for Aβ, a high initial brain uptake and rapid clearance from the brain are two important requirements. Therefore, biodistribution studies of [^{125}I]**2** and [^{125}I]**8** were performed in normal mice and expressed as % of injected dose per gram (%ID/g) (Table 2). [^{125}I]**2** showed a high initial uptake (4.82%ID/g at 2 min) and rapid clearance from the brain (0.45%ID/g at 60 min). On the other hand, [^{125}I]**8** showed a modest brain uptake (1.62%ID/g at 2 min) and relatively slow clearance from the brain (0.56%ID/g at 60 min). The ratio $\text{brain}_{2\,\text{min}}/\text{brain}_{60\,\text{min}}$ is considered to be an important index for the selection of the candidate compounds. The $\text{brain}_{2\,\text{min}}/\text{brain}_{60\,\text{min}}$ ratios of [^{125}I]**2** and [^{125}I]**8** were 10.7 and 2.9, respectively. It should be noted that [^{125}I]**2** had a comparable $\text{brain}_{2\,\text{min}}/\text{brain}_{60\,\text{min}}$ ratio in the normal mice brain with the clinically used Aβ probes, such as

[^{123}I]IMPY (13.7)[12,13] and [^{11}C]BF-227 (12.3)[28,29]. The difference in the *in vivo* properties among these probes may be partly explained by lipophilicity. Because the lipophilicity of **2** (clogP = 4.3, calculated using a ChemBioDraw Ultra 13.0) was between those of BF-227 (clogP = 3.85) and IMPY (clogP = 4.64), **2** may have preferable lipophilicity for penetration of the blood-brain barrier, whereas **8** has higher lipophilicity (clogP = 5.64), which might reduce the brain uptake and washout from brain. The initial uptake of [^{125}I]**8** in the liver was much higher than that of [^{125}I]**2**, while a comparable accumulation of [^{125}I]**2** and [^{125}I]**8** was observed in the lung and kidney. Both tracers showed increase of radioactivity in the stomach with time, but the uptake of [^{125}I]**8** was higher than that of [^{125}I]**2**. These results indicated that the deionidation of [^{125}I]**8** was faster than that of [^{125}I]**2** *in vivo*. However, no significant increase in blood radioactivity level of [^{125}I]**8** was observed over time. In addition, the mouse plasma samples obtained at 10 and 60 min post-injection of [^{125}I]**8** were analyzed by radio-TLC; the metabolites of [^{125}I]**8** were much more hydrophilic than the parent [^{125}I]**8** (data not shown). In general, blood-brain barrier penetration by very polar compounds is limited[30]. Therefore, the deiodination could have minimal effects on the brain accumulation of [^{125}I]**8**. However, it should be considered that the [^{125}I]iodoallyloxy group of [^{125}I]**8** was unstable *in vivo*. Novel ^{125}I labeled iodoalkenyl-substituted chalcone derivatives with improved *in vivo* pharmacokinetics and metabolic stability could be prospective Aβ imaging probes.

3. Conclusion

[^{125}I]**2** had a modest binding affinity for the Aβ aggregates and showed an unclear *in vitro* autoradiogram for the Aβ plaque, while its pharmacokinetic property was preferable for the *in vivo* brain imaging. Although the *in vivo* property of [^{125}I]**8** was unsuitable for the *in vivo* imaging, [^{125}I]**8** showed excellent binding affinity for the Aβ aggregates and detected Aβ plaques in the brain sections of both the *Tg2576* mouse and AD patient by fluorescence microscopy and autoradiography. Thus, it has been demonstrated that introduction of the iodoallyloxy group into the chalcone backbone effectively improved its binding affinity for Aβ plaques. Based on this study, further chemical modifications could provide useful Aβ imaging probes based on the chalcone backbone.

4. Experimental

4.1. General information

All reagents were commercial products and used without further purification unless otherwise indicated. Na[^{125}]I was obtained from MP Biomedicals (Costa Mesa, CA, USA). The ^{1}H NMR spectra were obtained using a Varian Gemini 300 spectrometer with TMS as the internal standard. The mass spectra were obtained using JMS－700N or JMS-T100TD instruments (JEOL, Japan). The HPLC analysis was performed by a Shimadzu HPLC system (LC-10AT pump with SPD-10A UV detector, λ= 254 nm). An automated gamma counter with

a NaI(Tl) detector (Perkin-Elmer, 2470 WIZARD^2) was used to measure the radioactivity. 4-Dimethylamino-4'-iodo-chalcone (DMIC) and [^{125}I]DMIC were prepared by the method in the literature[10]. The AD transgenic mice (*Tg2576*, C57BL6, APPsw) were purchased from Taconic Farms, Inc. All animals were supplied by the Tagawa Experimental Animal Laboratory (Nagasaki, Japan). The experiments with animals were conducted in accordance with our institutional guidelines and were approved by the Nagasaki University Animal Care Committee.

4.1.1 (*E*)-1-(4-Iodophenyl)-3-(4-methoxyphenyl)prop-2-en-1-one (1)

4-Iodoacetophenone (2.46 g, 10 mmol) and 4-anisaldehyde (1.2 mL, 10 mmol) were dissolved in 20 mL of ethanol. The mixture was allowed to stir for 15 min in an ice bath. A 30 mL aliquot of 10% aqueous potassium hydroxide solution was then slowly added dropwise into the reaction mixture. The reaction solution was allowed to stir at room temperature for 4 h. A precipitate was collected and washed with ethanol to provide 3.69 g of **1** (quant). ^{1}H NMR (300 MHz, $CDCl_3$) δ ppm: 7.85 (d, *J* = 8.1 Hz, 2H), 7.80 (d, *J* = 15.7 Hz, 1H), 7.74 (d, *J* = 8.1 Hz, 2H), 7.59 (d, *J* = 8.7 Hz, 2H), 7.34 (d, *J* = 15.7 Hz, 1H), 6.96 (d, *J* = 8.7 Hz, 2H), 3.86 (s, 3H).

4.1.2. (*E*)-3-(4-(2-Hydroxyethoxy)phenyl)-1-(4-iodophenyl)prop-2-en-1-one (2)

To a solution of compound **1** (120 mg, 0.34 mmol) in DMF (2 mL) was added 2-

chloroethanol (45 μL, 0.34 mmol) and K_2CO_3 (138 mg, 1.02 mmol). The mixture was heated at 80 ˚C for 13 h. After cooling the reaction mixture, the solvent was quenched by H_2O and extracted three times with EtOAc. The combined organic layer was washed with brine. After drying over Na_2SO_4, the solvent was removed and the crude product was chromatographed on silica gel with hexane/EtOAc= 1:1 to give **5** (70 mg, 52%) as a yellow solid. ^{1}H NMR (300 MHz, $CDCl_3$) δ ppm: 4.01 (t, *J* =4.5 Hz, 2H), 4.13 (t, *J* =4.8 Hz, 2H), 6.98 (d, *J* = 9.0 Hz, 2H), 7.38 (d, *J* = 15.6 Hz, 1H), 7.60 (d, *J* = 9.0 Hz, 2H), 7.74 (d, *J* =9.0 Hz, 2H), 7.76 (d, *J* = 15.6 Hz, 1H), 7.85 (d, *J* = 8.7 Hz, 2H). HRMS (FAB) *m/z* calcd for $C_{17}H_{16}IO_3$ (M^+) 395.014, found 395.014.

4.1.3. (*E*)-3-(4-(2-(2-Hydroxyethoxy)ethoxy)phenyl)-1-(4-iodophenyl)prop-2-en-1-one (3)

Using the above procedure for **2** starting from compound **1** and 2-(2-Chloroethoxy)ethanol (58 μL, 0.56 mmol), the title compound **3** (60 mg, 49 %) was obtained as a yellow solid. ^{1}H NMR (300 MHz, $CDCl_3$) δ ppm: 3.69 (t, *J* =5.1 Hz, 2H), 3.78 (t, *J* =5.1 Hz, 2H), 3.92 (t, *J* =4.5 Hz, 2H), 4.20 (t, *J* =4.5 Hz, 2H), 6.98 (d, *J* =9.0 Hz, 2H), 7.38 (d, *J* = 15.6 Hz, 1H), 7.59 (d, *J* = 8.7 Hz, 2H), 7.74 (d, *J* =8.1 Hz, 2H), 7.75 (d, *J* = 15.6 Hz, 1H), 7.85 (d, *J* = 8.4 Hz, 2H). HRMS (FAB) *m/z* calcd for $C_{19}H_{20}IO_4$ (M^+) 439.041, found 439.040.

4.1.4. (*E*)-3-(4-(2-(2-(2-Hydroxyethoxy)ethoxy)ethoxy)phenyl)-1-(4-iodophenyl)prop-2-

en-1-one (4)

Using the above procedure for **2** starting from compound **1** and 2-[2-(2-chloroethoxy)ethoxy]ethanol (50 μL, 0.34 mmol), the title compound 6 (28 mg, 17 %) was obtained as a yellow solid. ^{1}H NMR (300 MHz, $CDCl_3$) δ ppm: 7.85 (d, *J* = 8.7 Hz, 2H), 7.76 (d, *J* =15.6 Hz, 1H), 7.74 (d, *J* = 8.7 Hz, 2H), 7.58 (d, *J* = 9.0 Hz, 2H), 7.37 (d, *J* =15.6 Hz, 1H), 6.98 (d, *J* = 9.0 Hz, 2H), 4.18 (t, *J* = 5.1 Hz, 2H), 3.89 (t, *J* = 5.1 Hz, 2H), 3.70-3.76 (m, 4H), 3.62-3.66 (m, 4H). HRMS (FAB) *m/z* calcd for $C_{21}H_{24}IO_5$ (M^+) 483.067, found 484.065.

4.1.5. (*E*)-3-(4-(2-Hydroxyethoxy)phenyl)-1-(4-tributylstannylphenyl)prop-2-en-1-one (5)

A mixture of **2** (58 mg, 0.15 mmol), bis(tributyltin) (0.12 mL, 0.24 mmol) and $Pd(PPh_3)_4$ (8.4 mg, 7.27 μmol) in a mixed solvent (9.0 mL, 2:1 dioxane/triethylamine mixture) was stirred for 11 h under reflux. The solvent was removed, and the residue was purified by silica gel chromatography hexane/EtOAc= 2 : 1, which gave **5** (40 mg, 0.0717 mmol, 48 %) as an orange-colored oil. ^{1}H NMR (300 MHz, $CDCl_3$) δ ppm: 7.92 (d, *J* =7.8 Hz, 2H), 7.75 (d, *J* =15.9 Hz, 1H), 7.63 (d, *J* = 9.0 Hz, 2H), 7.46 (d, *J* = 15.9 Hz, 1H), 6.98 (d, *J* = 9.0 Hz, 2H), 4.13 (t, *J* = 4.8 Hz, 2H), 4.01 (t, *J* = 4.8 Hz, 2H), 1.52-1.58 (m, 9H), 1.31-1.35 (m, 9H), 1.07-1.13 (m, 9H), 0.87-0.92 (m, 9H), MS (FAB) *m/z* 559 [M^+].

4.1.6. (*E*)-3-(4-(dimethylamino)phenyl)-1-(4-(((E)-3-(tributylstannyl)allyl)oxy)phenyl)

prop-2-en-1-one (7)

To a solution of compound **6**[13] (25.0 mg, 0.094 mmol) in DMF was added NaH (24.6 mg, 1.05 mmol). To the mixture was added (*E*)-$Bu_3SnCH=CHCH_2OTs$[17] (83 mg, 0.174 mmol) in DMF and stirred at room temperature for 4 h. The mixture was quenched by saturated NH_4Cl and extracted three times with $CHCl_3$. The combined organic layer was washed with brine. The solvent was removed and the crude product was chromatographed on silica gel with hexane/EtOAc= 2:1 to give **7** (25 mg, 45%) as a yellow-ocher oil. ^{1}H NMR (300 MHz, $CDCl_3$) δ ppm: 8.01 (d, *J*= 9.0 Hz, 2H), 7.79 (d, *J*= 15.6 Hz, 1H), 7.55 (d, *J*= 9.0 Hz, 2 H), 7.36 (d, *J*= 15.6 Hz, 1 H), 6.98 (d, *J*= 8.7 Hz, 1 H), 6.70 (d, *J*= 9.0 Hz, 2 H), 6.38 (dt, *J*= 18.8, 3.1 Hz, 1 H), 6.17(d, *J*= 18.0 Hz, 2 H), 4.64 (d, *J*= 3.3 Hz, 2H), 3.04 (s, 6 H), 1.57-0.864 (27 H, m). MS (FAB) *m/z* 598 (M^+).

4.1.7. (*E*)-3-(4-(dimethylamino)phenyl)-1-(4-(((E)-3-iodoallyl)oxy)phenyl)prop-2-en-1-one (8)

To a solution of **7** (22.2 mg, 0.037 mmol) in $CHCl_3$ (5.0 mL) was added a solution of iodine in $CHCl_3$ (2.0 mL, 0.25 M) at room temperature. The mixture was stirred at room temperature for 30 min and a saturated $NaHSO_3$ solution (10 mL) was added. The mixture was stirred for 5 min and the organic phase was separated. The aqueous layer was extracted three times with $CHCl_3$. The organic layer was successively washed with saturated aqueous $NaHCO_3$

and brine, then dried over Na_2SO_4. The crude product was chromatographed on silica gel with hexane/EtOAc= 3:1 to give **8** (10.0 mg, 62%) as a yellow powder. ^{1}H NMR (300 MHz, $CDCl_3$) δ ppm: 8.02 (d, *J*= 6.4 Hz, 2H), 7.78 (d, *J*= 11.6 Hz, 1H), 7.53 (d, *J*= 5.9Hz, 2 H), 7.34 (d, *J*= 11.7 Hz, 1 H), 6.95 (d, *J*= 6.6Hz, 2 H), 6.80 (dt, *J*= 13.6, 6.0 Hz, 1 H), 6.70 (d, *J*= 6.2Hz, 2 H), 6.59 (d, *J*= 11.2 Hz, 1 H), 4.54 (d, *J*= 5.7 Hz, 2H), 3.05 (s, 6 H). HRMS (FAB) *m/z* calcd for $C_{20}H_{21}INO_2$ (M^+) 434.0617, found 434.0598.

4.2. Radioiodination

The ^{125}I-labeled compounds ([^{125}I]**2**, [^{125}I]**8**) were prepared from the corresponding tributyltin derivatives (**2** and **6**, respectively) by iododestannylation. Briefly, 3% H_2O_2 (50 μL) was added to a mixture of the corresponding tributyltin derivative (50 μg/50 μL EtOH), Na[^{125}]I (3.7-7.4 MBq, specific activity 81.4 GBq/μmol), and 1 M HCl (50 μL) in a sealed vial. The reaction was allowed to proceed at room temperature for 3 min and terminated by addition of satd. $NaHSO_3$aq (100 μL). After alkalization with 100 μL of satd. $NaHCO_3$aq and extraction with ethyl acetate, the extract was dried by passing through an anhydrous Na_2SO_4 column and evaporated to dryness. The crude products were purified by HPLC on a Cosmosil C18 column (Nacalai Tesque, 5C18-AR-Ⅱ, 4.6×250 mm) with an isocratic solvent of CH_3CN/H_2O (5:5 for [^{125}I]**2** and 6:4 for [^{125}I]**8**) at the flow rate of 1.0 mL/min. The retention time of [^{123}I]**2** and [^{123}I]**8** were 18 min and 30 min, respectively.

4.3. Binding assays using the aggregated A*β* peptide in solution

Binding assays by using filtration techniques were carried out as described previously[10]. A solid form of A*β*(1-42) was purchased from Peptide Institute (Osaka, Japan). Aggregation was carried out by gently dissolving the peptide (0.25 mg/mL) in a buffer solution (pH 7.4) containing 10 mM sodium phosphate and 1 mM EDTA. The solution was incubated at 37 ºC for 42 h with gentle and constant shaking. A mixture containing 50 μL of test compounds (8 pM–12.5 μM in 10% ethanol). 50 μL of 0.02 nM [^{125}I]DMIC, 50 μL of the A*β* aggregates, and 850 μL of 10% ethanol was incubated at room temperature for 3 h. The mixture was then filtered through Whatman GF/B filters using a Brandel M-24 cell harvester, and the filters containing the bound ^{125}I ligand were measured by an automatic gamma counter (PerkinElmer, 2470 WIZARD^2). Values for the half-maximal inhibitory concentration (IC_{50}) were determined from displacement curves of three independent experiments using GraphPad Prism 4.0, and those for the inhibition constant (K_i) were calculated using the Cheng-Prusoff equation.

4.4. Fluorescence staining on *Tg2576* mice brain sections

The *Tg2576* mice (female, 22-month-old) and wild-type mice (female, 22-month-old) were used as the Alzheimer's model and control mice, respectively. After the mice were sacrificed by decapitation, the brains were immediately removed and frozen in powdered dry

ice. The frozen blocks were sliced into serial sections, 10 μm thick. Each slide was incubated with a 50% DMSO solution (100 μM) of **2** and **8** for 3 h. The sections were washed in 50 % DMSO for 5 min twice. The fluorescence images were collected by BZ8100 (Keyence) using a DAPI-BP filter set (excitation, 360 nm; diachromic mirror, 400 nm; longpass filter, 460 nm) or a GFP-BP filter set (excitation, 470 nm; diachromic mirror, 495 nm; longpass filter, 535 nm). Thereafter, the serial sections were also stained with thioflavin S, a pathological dye commonly used for staining A*β* plaques in the brain, and examined using the microscope in the same condition with that of chalcones.

4.5. *In vitro* autoradiography on *Tg2576* mice brain sections

The brain sections of *Tg2576* mice (female, 22-month-old) were incubated in the 50 % DMSO solution containing [^{125}I]**2** or [^{125}I]**8** (3.7 kBq/150 μl, 0.3 nM) for 1 h. The slices were rinsed 5 min×3 each with a 60 % DMSO solution, and subsequently dipped into cold water (30 s). The sections were dried under a stream of cold air and placed in contact with the imaging plates (BAS-MS 2040; Fuji Film) for 24 h. The distributions of the radioactivity on the plates were analyzed by a Fluoro Image Analyzer (FLA5100; Fuji Film). Thereafter, the serial sections were also stained with thioflavin S. *In vitro* autoradiography of the postmortem brain slices were performed according to the above described method. The postmortem brain tissues from an autopsy-confirmed case of AD (73-year-old male) were obtained from BioChain Institute,

Inc. The presence and localization of plaques on the sections were confirmed by immunohistochemical staining using the monoclonal antibody BC05 (Wako) as already reported[31].

4.6. *In vivo* biodistribution in normal mice

A saline solution (100 μL) of [^{125}I]**2** or [^{125}I]**8** (7.4 kBq) was directly injected intravenously into the tail of ddY mice (5-week-old, 20–25 g). The mice were sacrificed at various times post-injection. The organs of interest were removed and weighed, and the radioactivity was measured by the gamma counter.

4.7. Statistical analysis

Statistical significance was determined at $p<0.05$ using the one way analysis of variance for comparison of more than two means, followed by post hoc tests using Bonferroni's correction.

Acknowledgments

Financial support was provided by a Grant-in-Aid for Scientific Research (B) (Grant No. 21390348) from Japan Society for the Promotion of Science (JSPS).

Reference

1. Querfurth, H. W.; LaFerla, F. M. *N Engl J Med.* **2010**, 362, 329.
2. Huang, Y.; Mucke, L. *Cell.* **2012**, 148, 1204.
3. Hardy, J.; Selkoe, D. J. *Science.* **2002**, 297, 353.
4. Mathis, C. A.; Mason, N. S.; Lopresti, B. J.; Klunk, W. E. *Semin Nucl Med.* **2012**, 42, 423.
5. Rowe, C. C.; Villemagne, V. L. *J Nucl Med Technol.* **2013**, 41, 11.
6. Vandenberghe, R.; Adamczuk, K.; Dupont, P.; Laere, K. V.; Chételat, G. *Neuroimage Clin.* **2013**, 2, 497.
7. Williams, S.C.P. *Nat Med*. **2013**, 19, 1551.
8. Cheng, Y.; Ono, M.; Kimura, H.; Ueda, M.; Saji H. *J Med Chem.* **2012**, 55, 2279.
9. Li, Z.; Cui, M.; Dai, J.; Wang, X.; Yu, P.; Yang, Y.; Jia, J.; Fu, H.; Ono, M.; Jia, H.; Saji, H.; Liu, B. *J Med Chem.* **2013**, 56, 471.
10. Qu, W.; Kung, M. P.; Hou, C.; Oya, S.; Kung, H. F. *J Med Chem.* **2007**, 50, 3380.
11. Qu, W.; Kung, M. P.; Hou, C.; Benedum, T. E.; Kung, H. F. *J Med Chem.* **2007**, 50, 2157.
12. Kung, M. P.; Hou, C.; Zhuang, Z.P.; Zhang, B.; Skovronsky, D.; Trojanowski, J.Q.; Lee, V.M.; Kung, H.F. *Brain Res.* **2002**, 956, 202.
13. Zhuang, Z. P.; Kung, M. P.; Wilson, A.; Lee, C.W.; Plössl, K.; Hou, C.; Holtzman, D. M.; Kung, H. F. *J Med Chem.* **2003**, 46, 237.

14. Kung, M. P.; Weng, C. C.; Lin, K. J.; Hsiao, I. T.; Yen, T. C.; Wey, S. P. *Chang Gung Med J.* **2012**, 35, 211.

15. Ono, M.; Yoshida, N.; Ishibashi, K.; Haratake, M.; Arano, Y.; Mori, H.; Nakayama, M. *J Med Chem.* **2005**, 48, 7253.

16. Ono, M.; Watanabe, R.; Kawashima, H.; Kawai, T.; Watanabe, H.; Haratake, M.; Saji, H.; Nakayama, M. *Bioorg Med Chem.* **2009**, 17, 2069.

17. Ono, M.; Hori, M.; Haratake, M.; Tomiyama, T.; Mori, H.; Nakayama, M. *Bioorg Med Chem.* **2007**, 15 6388.

18. Ono, M.; Haratake, M.; Mori, H.; Nakayama, M. *Bioorg Med Chem.* **2007**, 15, 6802.

19. Ono, M.; Watanabe, R.; Kawashima, H.; Cheng, Y.; Kimura, H.; Watanabe, H.; Haratake, M.; Saji, H.; Nakayama, M. *J Med Chem.* **2009**, 52, 6394.

20. Ono, M.; Ikeoka, R.; Watanabe, H.; Kimura, H.; Fuchigami, T.; Haratake, M.; Saji, H.; Nakayama, M. *ACS Chem Neurosci*. **2010**, 1, 598.

21. Ono, M.; Maya, Y.; Haratake, M.; Ito, K.; Mori, H.; Nakayama, M. *Biochem Biophys Res Commun.* **2007**, 361, 116.

22. Maya, Y.; Ono, M.; Watanabe, H.; Haratake, M.; Saji, H.; Nakayama, M. *Bioconjug Chem.* **2009**, 20, 95.

23. Ono, M.; Maya, Y.; Haratake, M.; Nakayama, M. *Bioorg Med Chem.* **2007**, 15, 444.

24. Zea-Ponce, Y.; Mavel, S.; Assaad, T.; Kruse, S.E.; Parsons, S.M.; Emond, P.; Chalon, S.;

Giboureau, N.; Kassiou, M.; Guilloteau, D. *Bioorg Med Chem.* **2005**, 13, 745.

25. Cui, M.; Ono, M.; Kimura, H.; Ueda, M.; Nakamoto, Y.; Togashi, K.; Okamoto, Y.; Ihara, M.; Takahashi, R.; Liu, B.; Saji, H. *J Med Chem.* **2012**, 55, 9136.
26. Cui, M.; Ono, M.; Kimura, H.; Liu, B.; Saji, H. *J Med Chem.* **2011**, 54, 2225.
27. Li, Z.; Cui, M.; Dai, J.; Wang, X.; Yu, P.; Yang, Y.; Jia, J.; Fu, H.; Ono, M.; Jia, H.; Saji, H.; Liu, B. *J Med Chem*. **2013**, 56, 471.
28. Kudo, Y.; Okamura, N.; Furumoto, S.; Tashiro, M.; Furukawa, K.; Maruyama, M.; Itoh, M.; Iwata, R.; Yanai, K.; Arai, H. *J Nucl Med.* 2007, 48, 553.
29. Okamura, N.; Shiga, Y.; Furumoto, S.; Tashiro, M.; Tsuboi, Y.; Furukawa, K.; Yanai, K.; Iwata, R.; Arai, H; Kudo, Y.; Itoyama, Y.; Doh-ura, K. *Eur J Nucl Med Mol Imaging.* **2010**, 37, 934.
30. Waterhouse, R. N. *Mol. Imaging Biol.* **2003**, 5, 376.
31. Kung, M. P.; Hou, C.; Zhuang, Z. P.; Skovronsky, D.; Kung, H. F. *Brain Res.* **2004**, 1025, 98.

Scheme 1. Synthesis of chalcone derivatives.

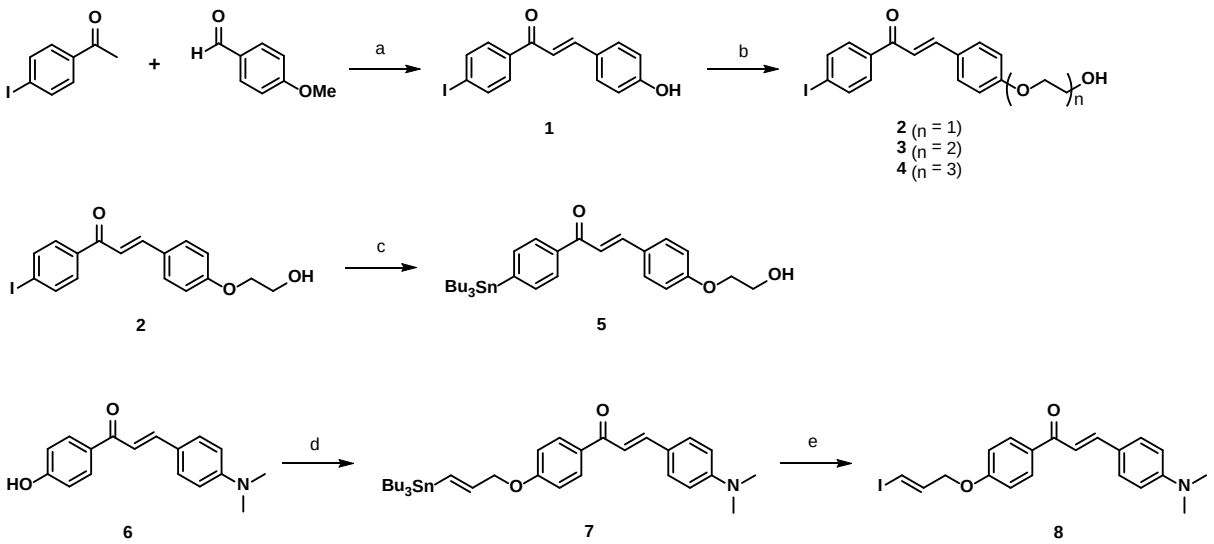

Reagents and conditions: (a) 10% KOH, EtOH, rt, 4 h; (b) $H(OCH_2CH_2)_nCl$, K_2CO_3, DMF, 80 ˚C, 13-15 h; (c) dioxane, $(Bu_3Sn)_2$, $(Ph_3P)_4Pd$, Et_3N, reflux, 11 h; (d) (*E*)-Bu_3SnCH=$CHCH_2OTs$, NaH, DMF, rt, 4 h; (e) I_2, $CHCl_3$, rt, 30 min.

Scheme 2. Radiosynthesis of ^{125}I labeled chalcone derivatives.

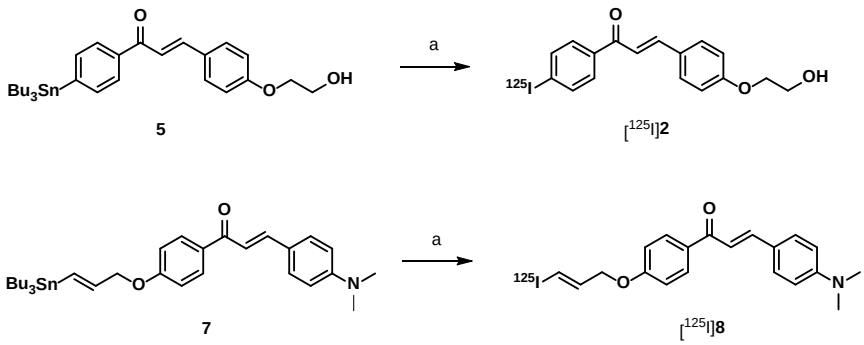

Reagents and conditions: (a) Na[^{125}]I, H_2O_2 , HCl, EtOH, rt, 3 min.

Table 1. Inhibition constant (K_i) of chalcone derivatives for Aβ aggregates.

Compounds	***K*i[a] (nM)**		
2	24.0	±	10.4
3	127.1	±	27.3
4	87.8	±	20.3
8	4.5	±	1.5
DMIC	10.8		0.9

[a] Inhibition constant (K_i) of chalcone derivatives were determined using [^{125}I]DMIC as a radioligand for Aβ aggregates. Each value (mean ± SEM) was determined by 3−6 independent experiments.

Table 2. Biodistribution of radioactivity after *i.v.* injection of ^{125}I labeled chalcone derivatives in normal mice.[a]

	Time after injection (min)			
Organ	2	10	30	60
		[^{125}I]**2**		
Blood	3.95(0.30)	3.01(0.58)	2.60(0.42)	2.27(0.60)
Liver	14.76(2.88)	20.11(4.81)	18.83(1.20)	15.57(3.17)
Kidney	10.34(1.72)	9.05(1.72)	10.23(1.96)	9.89(3.07)
Intestine	3.98(0.66)	10.55(3.41)	26.39(6.69)	25.16(6.54)
Spleen	2.69(0.54)	2.35(0.74)	1.21(0.10)	0.81(0.14)
Lung	7.14(1.34)	4.63(1.37)	3.21(1.24)	1.94(0.42)
Stomach	2.22(0.41)	3.38(2.38)	4.27(3.43)	4.01(0.38)
Pancreas	6.12(1.26)	3.37(1.00)	1.07(0.44)	0.90(0.54)
Heart	6.20(1.19)	3.13(0.88)	1.54(0.13)	1.05(0.32)
Brain	4.82(1.19)	2.86(0.87)	1.00(0.05)	0.45(0.09)
		[^{125}I]**8**		
Blood	2.65(0.21)	2.29(0.19)	1.97(0.55)	2.43(1.18)
Liver	23.21(2.52)	19.84(6.55)	16.91(0.62)	10.26(0.55)
Kidney	8.98(1.60)	6.06(0.57)	4.52(0.59)	4.17(1.12)
Intestine	1.74(0.59)	2.38(0.88)	4.45 (1.70)	6.34(2.57)
Spleen	4.43(1.11)	5.34(2.03)	4.68(1.31)	3.92(1.52)
Lung	8.08(1.39)	4.48 (0.38)	3.16(0.42)	3.28(1.01)

Stomach	2.49(1.07)	5.19(2.16)	8.98(5.05)	16.44(6.82)
Pancreas	4.02(1.48)	3.27(0.51)	2.35(0.63)	2.14(1.12)
Heart	8.70(1.66)	3.39(0.38)	2.20(0.13)	2.10(0.85)
Brain	1.62(0.30)	1.63(0.22)	0.87 (0.18)	0.56(0.16)

[a] Expressed as % of injected dose per gram (%ID/g). Each value represents mean (SD) for 5 or 6 mice at each interval.

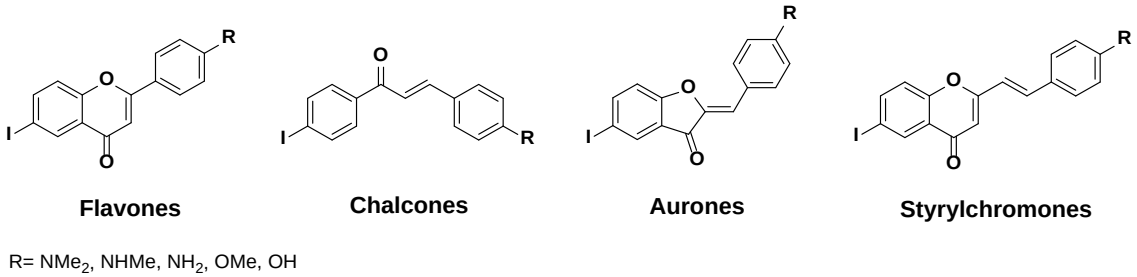

R= NMe_2, NHMe, NH_2, OMe, OH

Figure 1. Chemical structures of flavonoid derivatives reported as amyloid imaging probes.

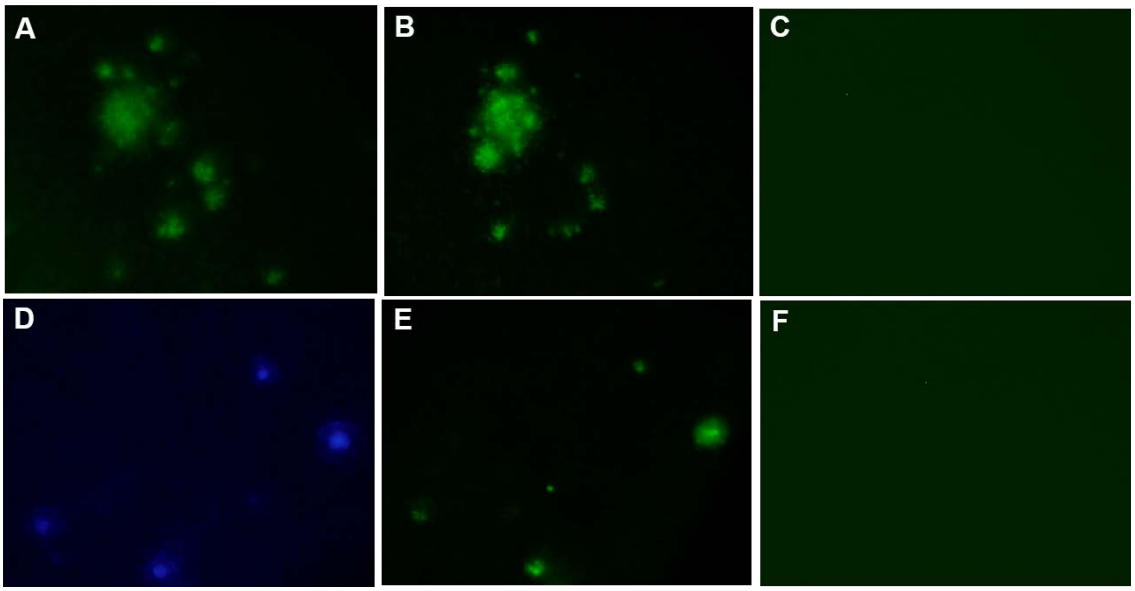

Figure 2. Neuropathological staining of chalcone derivatives **2** (A) and **8** (D) in 10 μm sections of *Tg2576* mice brain. Labeled plaques were confirmed by staining of the adjacent sections with thioflavin-S (B and E). Fluorescence images of **2** (C) and **8** (F) in the age-matched control mouse brain sections.

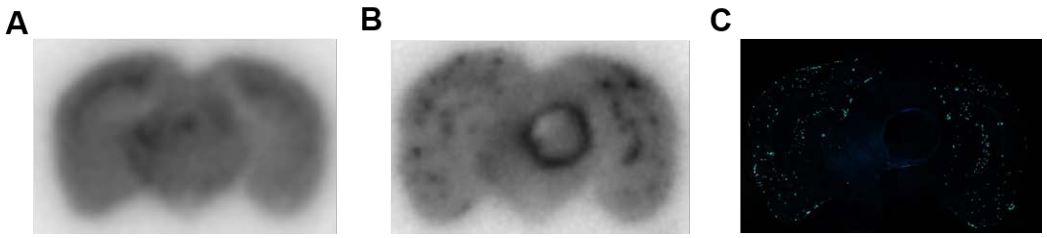

Figure 3. *In vitro* autoradiograms of chalcone derivatives [^{125}I]**2** (A) and [^{125}I]**8** (B) in the brain sections of *Tg2576* mouse brain. Fluorescence image of thioflavin-S in the adjacent section (C).

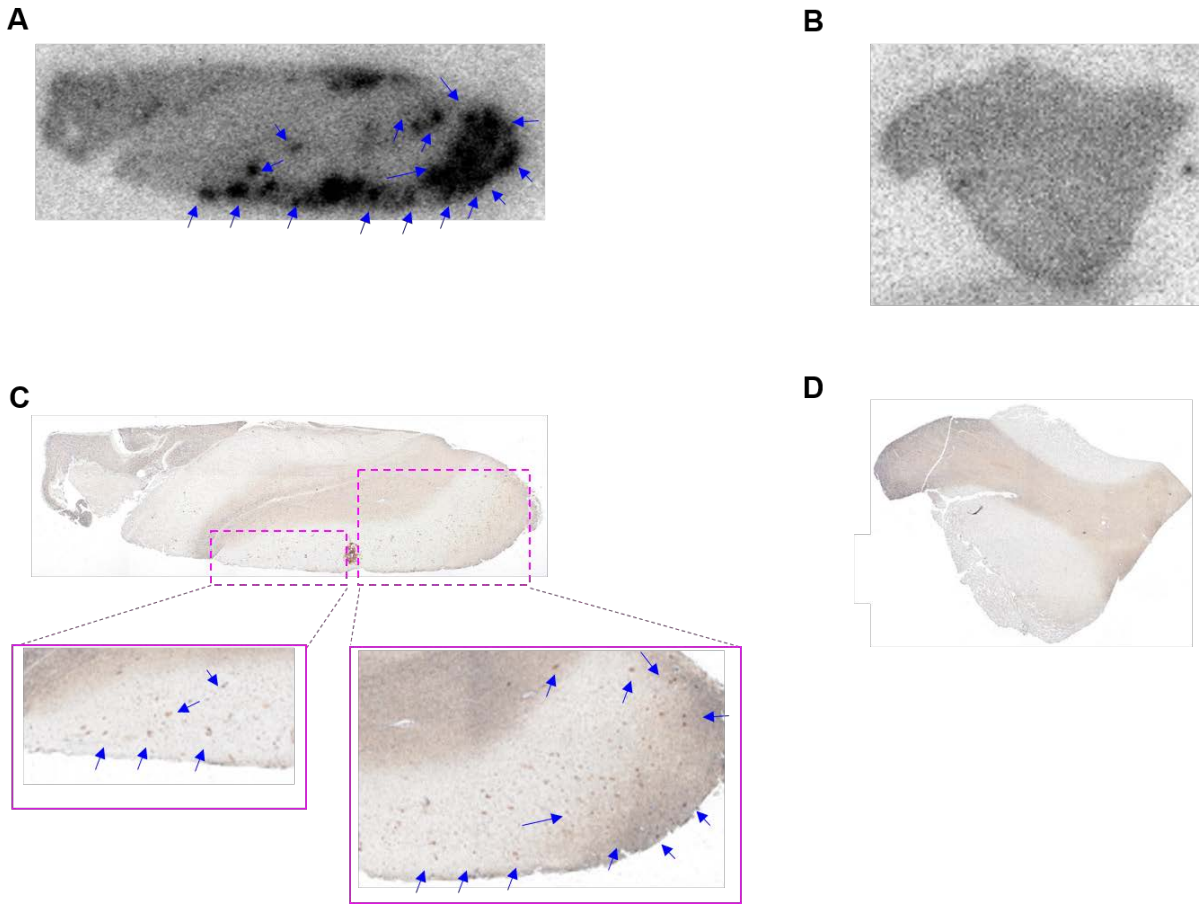

Figure 4. *In vitro* autoradiographic images of [^{125}I]**8** in the hippocampal (A) and frontal lobe (B) sections of AD patient (73-year-old male). Immunohistochemical staining of each section using a monoclonal anti-Aβ antibody (C and D, respectively).